Robotica (2010) volume 28, pp. 893–907. © Cambridge University Press 2009
doi:10.1017/S0263574709990725

Analysis of typical locomotion of a symmetric hexapod robot

Z.-Y. Wang*,§,¶, X.-L. Ding§ and A. Rovetta¶

§*Robotics Research Institute, Beijing University of Astronautics and Aeronautics, Beijing 100083, China*
¶*Department of Mechanical Engineering, Politecnico di Milano, Via Lamasa 34, Milan 20156, Italy*

(Received in Final Form: November 11, 2009. First published online: December 23, 2009)

SUMMARY

In recent years hexagonal hexapod robots gained the interest of international research community. The aim of this paper is twofold. First, after summarizing all known gaits of such robots, we introduce some improvements both for normal conditions and for fault tolerance. Then we show the advantages of hexagonal hexapod robots over rectangular ones by comparing different gaits from theoretical and experimental points of view. Stability, fault tolerance, turning ability, and terrain adaptability are analyzed. For reaching these aims we also introduce a robot kinematics that considers at the same time supporting and transferring legs. The trajectories of feet are described as well. Finally, single leg stride selection is studied for side wave and for kick-off gaits to optimize walking ability and energy management.

The theoretical results presented herein have been validated with experiments conducted on a prototype of the Novel Robotics System for Planetary Exploration (Rovetta *et al.,* "New Robot Concepts for Mars Soil Exploration: Mechanics and Functionality," *ASTRA 2004, Eighth ESA Workshop on Advanced Space Technologies for Robotics and Automatian,* Nordwijk, The Netherlands Nov. 2–4, 2004) (NOROS), developed by Politecnico di Milano and Beijing University of Astronautics and Aeronautics, and the results are summarized in this paper.

KEYWORDS: Hexapod robot; Locomotion, Symmetric; Trajectory; Agility.

1. Introduction

Multilegged robots display significant advantages with respect to wheeled ones for walking over rough terrain because they do not need continuous contact with the ground. In nature, most arthropods have six legs to easily maintain static stability, and it has been observed that a larger number of legs does not increase walking speed.[2] Moreover, hexapod robots show robustness in case of leg faults.[3–10] For these reasons, hexapod robots have attracted considerable attention in recent decades. The most studied problem for multilegged robots concerns how to determine the best sequence for lifting off and placing the feet (gait planning) while many results have been obtained on this topic, the field is still open to research.

* Corresponding author. E-mail: zhiying.wang@mail.polimi.it

Gait is a key element for multilegged robots and it is solely dependent on the design of bodies and legs. Hexapod gaits have been widely investigated as a function of shape and characteristics of the robot structure. In 1985, Kaneko *et al.*[11] addressed the gait of a rectangular hexapod with decoupled freedoms where the propelling motion was generated by one degree of freedom (DOF). In 1988, Lee *et al.*[12] realized an omnidirectional walking control system for a rectangular hexapod robot with adaptive suspension. A circular gait was studied for a layered hexapod robot (called Ambler) at the Carnegie Mellon University[10,13–14] with rotating legs connected to the same vertical axis at six different heights. Hirose *et al.*[15–16] and Gurocak[17] developed other two hexapods whose bodies were consisting of two different layers, each connected to three legs. The relative motion of the layers realized the omnidirectional robot gait in a simple way, but limiting the walking capability under leg faults. Lees[18] studied the gait of a special robot whose body was composed of three parts connected by revolute joints. Its flexible gait allowed it to overcome complex terrains, but its configuration was quite complicate for control system design R Hex, introduced by Saranli *et al.*,[19] is another hexapod robot with half-circle legs with a simple alternate tripod gait.

Most popular hexapods can be grouped into two categories, rectangular, and hexagonal ones. Rectangular hexapods have a rectangular body with two groups of three legs distributed symmetrically on the two sides. Hexagonal hexapods have a round or hexagonal body with evenly distributed legs. A typical leg has three DOFs.

The gait of rectangular six-legged robots has motivated a number of theoretical researches and experiments which nowadays reached to some extent a state of maturity. Lee *et al.*[20] showed for rectangular hexapods the longitudinal stability margin, which is defined as the shortest distance from the vertical projection of center of gravity to the boundaries of the support pattern in the horizontal plane, of straight-line motion and crab walking. Song *et al.*[21] defined the duty factor β as the fraction of cycle time in which a leg is in the supporting phase and they proved that the wave gait is optimally stable among all periodic and regular gaits for rectangular hexapods when $3/4 \leq \beta < 1$. Both the tripod gait and the problem of turning around a fixed point on an even terrain have been widely investigated and tested for a general rectangular hexapod with three DOF legs.[22,23] The so called 4+2 quadruped gaits[24] have been demonstrated being able to tolerate faults.[6] A series of fault-tolerant gaits for hexapods were analyzed by Yang *et al.*[3–7] Their aim was

to maintain the stability in case a fault event prevented a leg from supporting the robot. Kugushev and Jaroshevskij[25] proposed a terrain adaptive free gait that was nonperiodic. McGhee *et al.*[26] and other researchers[27,28] went on studying free gaits of rectangular hexapod robots.

At the same time, the hexagonal hexapod robots were studied with inspiration from the insect family, demonstrate better performances for some aspects than rectangular robots. Kamikawa *et al.*[29] confirmed the ability to walk up and down a slope with the tripod gait by building a virtual smooth surface that approximates the exact ground. Yoneda *et al.*[30] enhanced the results of ref. [21], developing a time-varying wave gait for hexagonal robots, in which velocity, duty factor, and crab angle are changed according to terrain conditions. Preumon *et al.*[2] proved that hexagonal hexapods can easily steer in all directions and that they have longer stability margin, but he did not give a detailed theoretical analysis. Takahashi *et al.*[9] found that hexagonal robots rotate and move in all directions at the same time better than rectangular ones by comparing stability margin and stroke in wave gait, but no experimental results were presented. Chu and Pang[31] compared the fault-tolerant gait and the 4+2 gait for two types of hexapods of the same size. They proved theoretically that hexagonal hexapod robots have superior stability margin, stride, and turning ability compared to rectangular robots.

It is also worth to mention here a work carried out by P. Gonzale de Santos *et al.*[32–33] They optimized the structure of rectangular hexapods and found that extending the length of middle legs of rectangular robots helps in saving energy. This outcome can be seen as a transition from rectangular six-legged robots to hexagonal ones.

To date many studies have been given for different hexapod locomotion. However a comprehensive comparison among different gaits and between rectangular and hexagonal hexapods does not appear to have been published. The topic is still a subject of research and new gaits can be found.

This paper focuses on a typical six-legged hexagonal robot with three-DOF legs. First, a summary of the gaits for such robots is presented, and then they are compared with those of general rectangular six-legged. An extensive study is performed with new types of gaits, and comparative studies on stability and ability in avoiding obstacles are carried out. Fault-tolerant gaits are discussed for the cases of rupture of one leg or two legs. In the literature, it appears that only opposite damaged legs are treated. Here, we tackle also the failure of two adjacent legs and two separated by one normal leg. Other aspects of hexapod robots' locomotion such as surmounting obstacles and climbing slope are probed as well. To facilitate simulations and experiments, we provide new kinematics in which the coupling effect of swing legs on supporting legs is considered. Finally, stride selection is analyzed from the mathematical point of view. Most the gaits discussed herein have been tested with a NOROS prototype, which is an improved version of the double-locomotion (wheel and leg) model "Ladyfly."[34–36] The Ladyfly robot was developed in 2003 within a project of space robotic exploration, devoted to Mars and Moon. It was first presented in ref. [37], among a group of projects dealing with "intelligence in space robotics." The wheel system of NOROS is not analyzed in the present paper.

(a) Robot

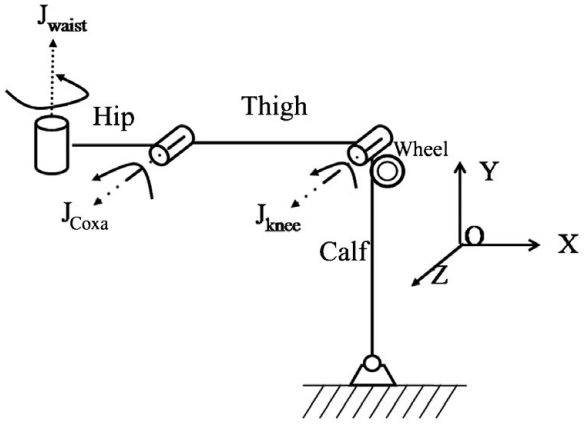

(b) Leg

Fig. 1. NOROS robot structure.

The paper is organized as follows. Section 2 simply addresses the structure and physical parameters of NOROS robot. In Section 3, normal gaits of hexagonal hexapods are summarized and analyzed. In Section 4 fault-tolerant gaits for hexapods are proposed Section 5 concerns the ability to walk over rough terrain. In Section 6, the trajectories of feet tips are provided and simulated experiment and simulation results of discussed gaits based on the NOROS robot are presented in Section 7. Finally, conclusions are drawn.

2. Structure Of NOROS Robot

Lunar robots have become a hot topic in recent years. The lunar surface is covered with a thick layer of dust (called regolith) and unknown obstacles that make wheeled locomotion difficult. The NOROS robot (Fig. 1a) has six legs which are suitable for walking on such soft soil. It has also wheels on each leg to achieve high speeds when hard smooth surfaces are encountered. The body of the NOROS robot is a hemispherical shell, inside which electronic circuitry, communication systems and control hardware are housed. Its six legs are distributed evenly around the shell. The structure of a single leg is as in Fig. 1(b). It consists of three elements: hip, thigh and calf, connected together by two parallel revolute joints, coxa and knee, with rotating

Table I. Main physical parameters of designed NOROS robot.

	Each leg			
	Hip	Thigh	Calf	Body
Mass (kg)	$m_1 = 0.80$	$m_2 = 2.00$	$m_3 = 2.00$	$m_b = 10.9$
Length (m)	$l_1 = 0.09$	$l_2 = 0.30$	$l_3 = 0.30$	$r_b = 0.36$

axes parallel to the ground. The hip is then connected to the body by the waist joint that rotates around a vertical axis.

Main parameters of the new designed NOROS, which will be used for subsequent analysis and simulation, are listed in Table I.

Similar to other references,[3–7,31] several assumptions concerning gaits and kinematics of the hexapod are made for the analysis carried out in the subsequent sections:

(1) Point contact between foot and ground;
(2) No slipping between foot and ground;
(3) Known special starting foothold positions.

3. Normal Gaits

Beside the free gait,[25–28] a hexapod robot has several types of periodic gait. Normally, it can walk with the tripod "3+3" type of gait, "4+2" type of gait and "5+1' gait.

3.1. "3+3" tripod gait

The tripod continuous gaits are characterized by having three legs standing on the ground for supporting and pushing the body forward, and the other three legs lifting off and swinging forward. In each gait period, the body moves two steps. The duty factor β[21] is 1/2.

According to current studies, the hexagonal hexapod robot has two periodic tripod gaits similar to that of rectangular robots The first one is the insect wave gait which is characterized by a forward wave of stepping actions on each side of the body with a half-cycle phase shift between the two members of any right or left pair.[26] In Fig. 2(a) a scheme of the robot is sketched, where the main direction of the movement, defined as main walking direction, as shown is upwards, with legs moving in groups of three swing forward. The second one is the mammal kick-off gait where legs generally move in a vertical plane like human's walking and trajectories of feet are along legs. The robot is depicted in Fig. 2(b), and it walks mainly from left to right like a crab.

In the following Figs. 3 and 4, 'R' and 'S' denote respectively. revolute and spherical joint, subscript 'f', 'k', 'c,' and 'w' denote '*foot*', '*knee*', '*coxa*,' and '*waist*', respectively. For instance, 'R_c' specifies that the coxa is a revolute joint; 'S_f' tells that between foot and ground, a virtual spherical joint is assumed

In the insect wave gait, the waist joints are the most active joints during walking, and each foot needs three DOFs. The connection between each foot and the ground can be considered as a spherical joint (S_f in Fig. 3).

In the mammal kick-off gait, the waist joints do not move during straight line walking. The connection between a foot and the ground can be considered as revolute joints (R_f in Fig. 4a). This structure can be simplified as in Fig. 4(b). For

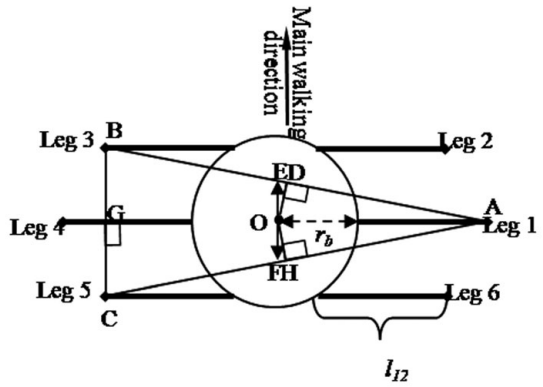

(a) Insect-wave tripod gait (ΔABC denotes the supporting area, l_{12} denotes legnth sum of hip and thigh)

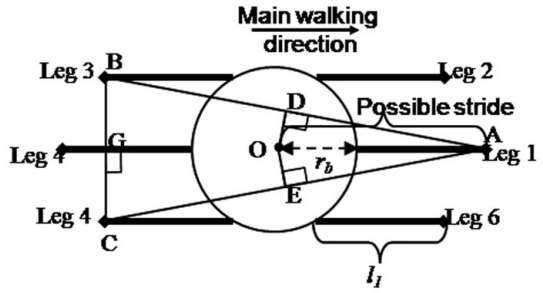

(b) Mammal kick-off tripod gait (ΔABC denotes the supporting area, l_{12} denotes legnth sum of hip and thigh)

Fig. 2. Natural tripod gaits.

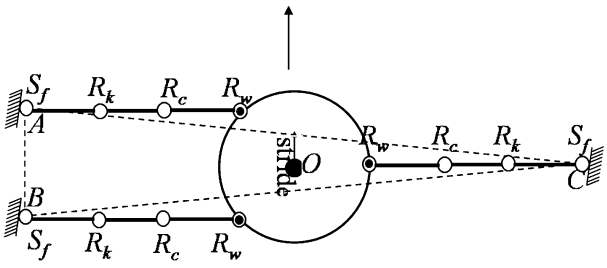

Fig. 3. Simplified structure of insect gait.

the closed chain including supporting legs, body and ground, the number of DOF F is 3. Only when the robot needs to turn, the waist joints become active and rotate to change direction.

In addition to the periodic tripod gaits mentioned above, we introduce here new type of mixed gait. During walking, the mixed gait has a supporting area in the form of an equilateral triangle (ΔABC or ΔDEF in Fig. 5). The dark point in Fig. 5 is the gravity center of the body. In every half period, one leg walks as in the mammal gait and two legs walk as in the insect gait. Between feet and ground there are one revolute and two spherical joints. The number of DOF of the mixed gait is 4. Figure 6 describes the walking sequence of the mixed gait

In ref. [21], it was claimed that a hexapod insect wave gait has the optimum stability among all hexapod periodic and regular gaits in the range of $1/2 < \beta < 1$. While this is true for rectangular hexapod robots, it does not hold for hexagonal ones

From Fig. 2 to Fig. 6, it is can be seen that, for a given robot, the insect wave gait has the same size of supporting

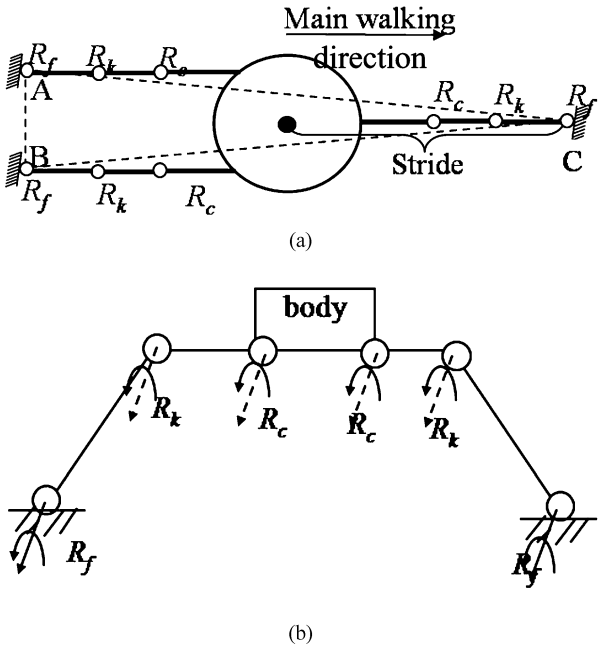

(a)

(b)

Fig. 4. Mammal gait.

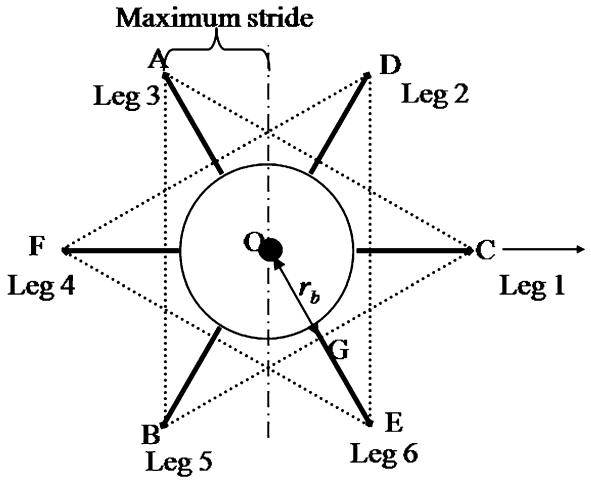

Fig. 5. Mixed gait.

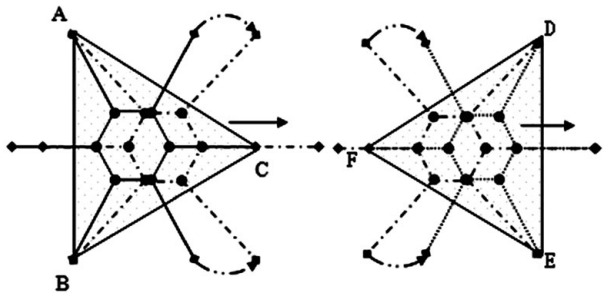

Fig. 6. Mixed gait sequence.

area ΔABC as the mammal gait; on the other hand, the mixed gait has the largest supporting area. We can now characterize the steps a robot can place.

Along the main walking direction (Fig. 2 and Fig. 3), we call kinematics margin the maximum stride a robot can reach due to its physical conditions (structure and length of legs, flexibility of joints, etc); define then the stability margin as the longest step the robot can stretch without losing stability. Given a robot and its initial state, we define r_b as the body radius and l_{l2} as the leg length (Fig. 2). Assuming that the robot's body moves in a plane at a constant height from the ground, the maximum strides for the three gaits are calculated and shown in Table II. Parameters are from Table I.

Table II. Maximum stride of tripod gait of hexagonal hexapod along main walking direction.

	Maximum stride along main walking direction		
	Stability margin formula	Stability margin for designed NOROS	Kinematics margin for designed NOROS
Insect gait	$\frac{\sqrt{3}r_b(r_b+l_{12})}{4l_{12}+3r_b}$	14.57 cm	>20 cm
Mammal gait	r_b+l_l	69 cm	21.96 cm
Mixed gait	$\frac{r_b+l_{12}}{2}$	34.5 cm	20.75 cm

From Table II we see that a hexagonal hexapod such as NOROS walking with the insect gait has a stability margin shorter than its kinematics margin therefore there is a possibility for loss of stability. Whereas the mammal and mixed gaits can guarantee static stability with any feasible stride, while the mammal gait has a slight longer maximum feasible stride because of kinematics limitation. From the control point of view, for straight line main direction walking, the simplest gait is the wave gait where all legs have the same trajectory, while the most complex is the mixed gait. However, the mixed gait has a higher statically stability-margin defined as the minimum distance from the gravity center of body to each edge of the supporting polygon

Concerning turning ability, the insect wave gait needs a special gait,[1,22,24,31] while the mammal gait turns through a small angle by adjusting all waist joints at the same time, and does not need a special transition period except for large angle turning. The mixed gait can turn through a large angle by adjusting the heading leg. For example, assume initially the walking angle is 0° while the leading led is leg 1 (Fig. 5) and the leg groups are 1+3+5 and 2+4+6 Then the robot will make a 60° turn if the leading leg is changed to leg 2.

Experimental results will be presented in Section 4 later concerning the turning capabilities of these three gaits.

3.2. "4+2" gait

The rectangular hexapod robot has another type of gait, the "4+2" gait.[31] For this gait the legs are grouped into three groups. Every time there are four legs (two groups) standing on the ground to support the body, two other legs rise and walk ahead. In one gait period, there are three steps and the body moves only one step. The duty factor is 2/3. The hexagonal six-legged robot also has this gait with same leg sequences as that of a rectangular hexapod,

This gait shows fault-tolerant ability under certain conditions,[4,6,24,31] because three legs can support the body even if one supporting leg broken during walking. Chu and Pang[31] had proved that the hexagonal robot by this gait has

advantages compared with rectangular ones in stability, stride and turning ability, if the turning angle is within $[-30^\circ, 30^\circ]$.

3.3. "5+1" one by one gait

The robot can also move its legs one by one. This gait displays higher fault tolerance than the gaits discussed above. However, the duty factor is only 5/6 so that the efficiency is very low. This gait is just used for special movement, such as rotating the body, walking over highly irregular terrain, and avoiding big obstacles and so on.

3.4. Transition between different gaits

Many hexapod robots use only one type of the aforementioned gaits. Some references discuss more than one gait, but few considered how to transition from one to another. the transitions may be straightforward to implement, it still worth a comparison here.

Among tripod gaits, just two steps are required to transition from one to another because tripod gaits have two steps in each gait period. Figure 7 is an example of transition from the mammal tripod gait to the mix tripod gait. Dashed lines denote the swinging legs, solid lines denote supporting legs.

From "3+3" tripod gait to "4+2" quadruped gait, three steps are needed, the body just moves once, while from "4+2" to "3+3" two steps are needed and the body also moves once.

4. Fault-Tolerant Gaits

In arduous operating environments, robots may confront accidents and damage their legs; their legs may be dual-used as arms for some tasks, or some joints may suffer loss of control, etc. In such cases, biped or quadruped robots would become statically unstable However hexapods may still walk with static stable because their six legs provide redundancy. In this subsection we discuss these fault-tolerant gaits.

4.1. Joint lock

In this case, Yang[5] has already proposed a discontinuous tripod gait for rectangular hexapod robots

However, with joint-lock a hexagonal hexapod may still maintain a continuous gait. The three possibilities for a single locked joint on one leg are discussed in the following:

(1) Waist joint lock. In this case, the faulty leg cannot move in a horizontal plane, but it can swing in a vertical plane. The insect wave gait is difficult for this situation; whereas the mammal gait is still available by adjusting the other legs in parallel with the faulty leg. Also the mixed gait is possible if we chose the broken leg as the leading leg, or the leg opposite as healing leg.

(2) Knee or coax joint lock. For these two cases, the mammal gait and mixed gait are impossible to realize, but the insect gait is feasible, although not as efficient as before injury. If one whole leg is locked, the discontinuous tripod gait can be employed.

4.2. Loss of one leg

In the case of loss of one leg is due to fault or use for other tasks; two possibilities were considered in ref [4].

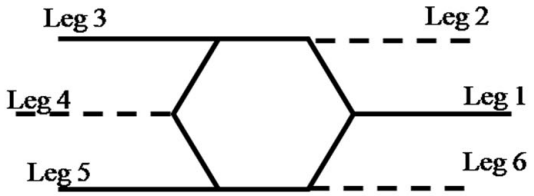

(a) Initial state: leg 2,4 and 6 raised, leg 1,3 and 5 support the body and push the body forward

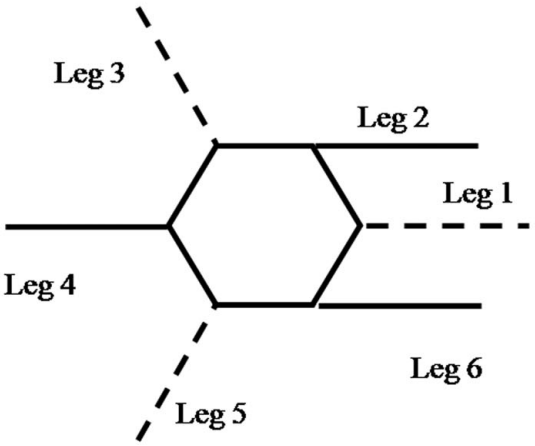

(b) The first step, raise leg 1, 3 and 5,adjust leg 3 and 5 to $\pm 120^o$ respectively while leg 2, 4 and 6 support and move the body with mamma gait.

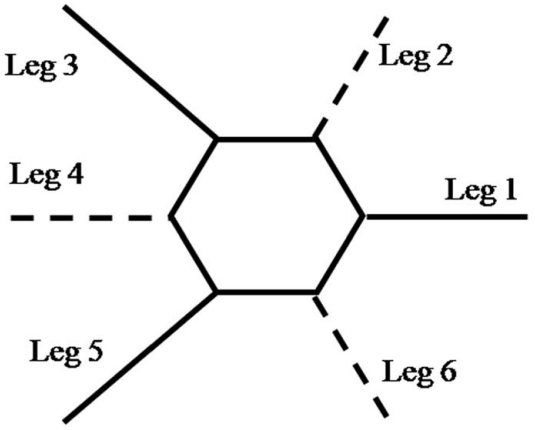

(c) The second step, raises leg 2, 4 and 6, adjust leg 2 and 6 to $\pm 60^o$ respectively. Leg 1, 3 and 5 support the body with mixed gait and push body forward.

Fig. 7. Transition sequence from mammal tripod to mix tripod.

However, for symmetric hexagonal robot, there is only one case because the structure of every leg is the same and distributed evenly around the body. The 2+1+2 gait has same sequence as ref. [4]. The difference is in the positions the leg.. The legs of the the gaits in ref. [4] are overlapping. The symmetrical hexapod robot needs three steps to achieve this walk. During this procedure, the robot's body moves two steps.

4.3. Loss of two legs

There are three cases where two legs are either faulty or being used for other tasks. The positions of these two unavailable legs may be opposite, adjacent or separated-by-one (two damaged separated by one normal leg). Some studies[9] have

been done in the first case, but there is a lack of study on the other two cases:

(1) The opposite-legs case. Losing two opposite legs, for example, leg i and leg j the hexapod robot becomes a quadruped robot. It can walk with one of quadruped gaits which have been widely studied. For example, the craw gait (Chen *et al.*[38]), the diagonal gait (Hirose[39]), mammal-type "3+1"gait (Tsujita *et al.*[40]), "3+1"craw gait (McGhee *et al.*[26] and Chen[41]) which maintains static stability at each step, and the omnidirectional updated quadruped free gait in refs. [42, 43].

(2) The two-separated-by-one case and adjacent case. For these two cases the two unavailable legs are on the same side therefore it is almost impossible for a general rectangular hexapod robot to have statically stable locomotion. For a hexagonal robot the insect wave periodic gait is still available. The other four legs can be adjusted to suitable initial positions, as shown in Fig. 8 for example. Figuer 8(a) is the case of losing leg 1 and leg 3. Fig. 8(b) shows the case where leg 1 and leg 2 are unavailable. Following the four-leg periodic gait sequence, robots can realize statically stable walking. The crab angle will be different For example, if leg 1 and leg 2 or leg 1 and leg 3 are unusable, the crab angle will be $-\pi/6$ as shown in Fig. 8. Figure 9 lists the leg sequences for a separated-by-one fault-tolerant gait. At each instant, there are three or four legs supporting the body. The mass center is inside the supporting area.

For the adjacent case, the leg sequence is similar to the separated-by-one case after adjusting to suitable initial positions.

To realize statically stable walking, there are several requirements in Fig. 8:

(1) $\overline{AE} = \overline{BF} = \overline{CG'} = \overline{DH'} = L$;

(2) $L \geq R\cos(\frac{\pi}{3})$;

(3) $\overline{GG'} = \overline{HH'} = s$, the body stride;

(4) $s < \overline{G'O_2} = \overline{O_2H'}$;

(5) $\overline{EO_1} = \overline{O_1F} = \overline{O_2G'} = \overline{O_2H'} = R\sin(\frac{\pi}{3})$

The rules for the quadruped insect wave gait are:

(1) Rear legs (leg 4 and leg 5 in Fig. 9) must not cross the central line (the point-dashed line in Fig. 8) while moving ahead, so that the mass center will also be in the subsequent supporting area.

(2) Front legs (leg 1 and leg 2 in Fig. 9) should not go back to the central line while the body (center of mass) is moving ahead.

(3) The stride of the swing legs is twice that of the body.

Setting the body reference frame as in Fig. 10, where X_o is parallel to the initial direction of hip 1; axis Y_o is parallel to the ground, Z_o is obtained according to right hand rule. From the initial position (Fig. 10) to the fault-tolerant initial state (Fig. 8), we can adjust the legs according to following procedures (Eqs. (1)–(10))

If two faults occur on two legs that separated by one, for example leg 1 and leg 3 the following procedure can be used to move the other legs from the original initial positions to the fault-tolerant initial positions:

Leg 2 moves from P_2 to F with stride $\overline{P_2F}$ (Eq. (1)) and rotates by angle θ_2(Eq. (2)) ; Leg 4 moves from P_4 to E with stride $\overline{P_4E}$ (Eq. (3)) and rotates by angle θ_4(Eq. (4)) ; Leg 5 moves from P_5 to G with stride $\overline{P_5G}$ (Eq. (5)) and rotates by angle θ_5 (Eq. (6)); Leg 6 moves from P_6 to F with stride $\overline{P_6H}$ (Eq. (7)) and rotates by angle θ_6(Eq. (8)):

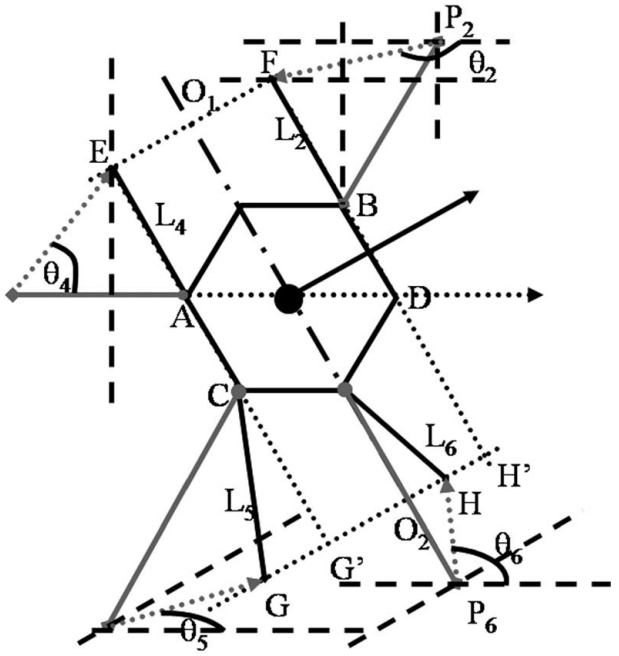

(a) Separated-by-one case (leg 1 and leg 3 are lost)

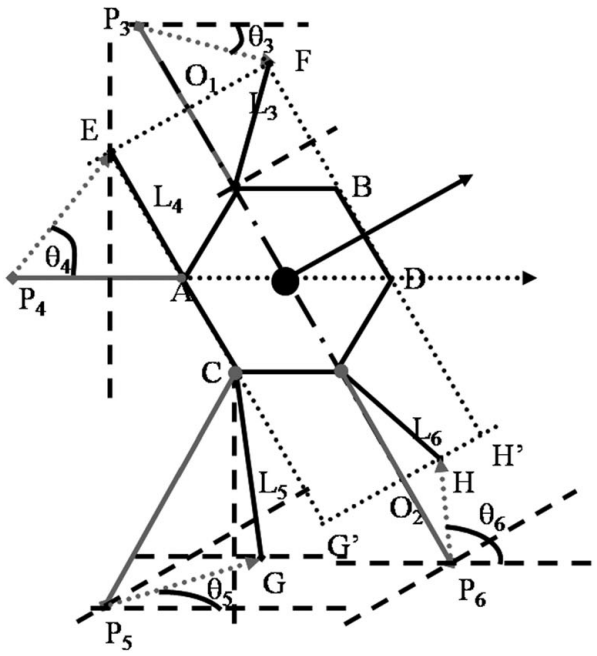

(b) Adjacent case (leg 1 and leg 2 are lost)

Fig. 8. Transition sequence from mammal tripod to mix tripod.

$$\overline{P_2F} = \sqrt{\left(L\sin\left(\frac{\pi}{3}\right)\right)^2 + \left(L - (l_1 + l_2)\cos\left(\frac{\pi}{3}\right)\right)^2}, \tag{1}$$

$$\theta_2 = a\tan\left(\frac{L - (l_1 + l_2)\cos(\frac{\pi}{3})}{L\sin(\frac{\pi}{3})}\right) - \frac{\pi}{6}, \tag{2}$$

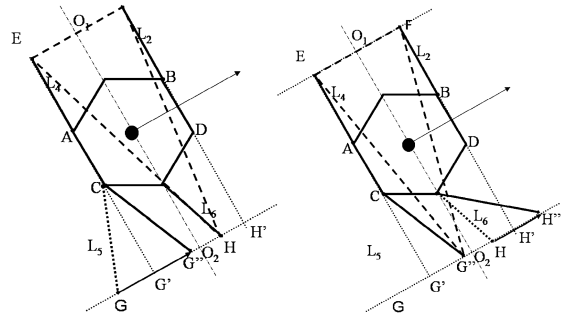

(a) (1) Swing rear right leg, leg 5;Supporting area is Δ EFH; (2) Swing front right leg, leg6 Supporting area is Δ EFG".

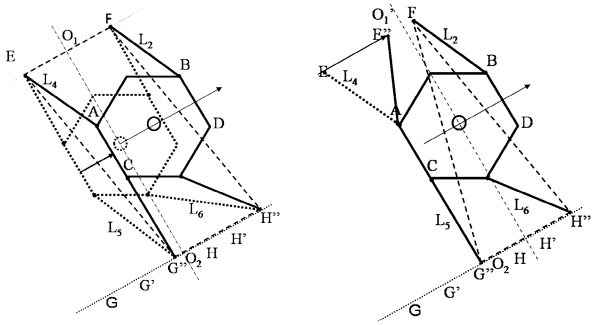

(b) (3) Move body;Supporting area is □ EFG"H"; (4) Swing rear left leg, leg4; Supporting area is Δ FG"H".

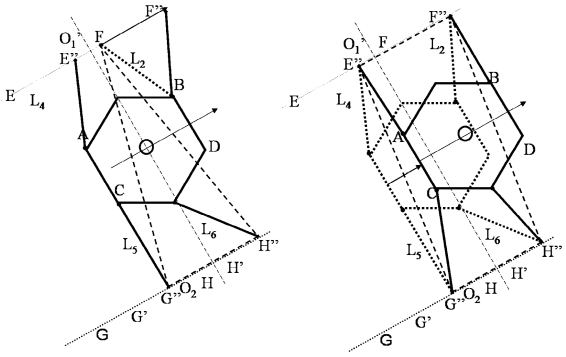

(c) (5) Swing front left leg, leg2;Supporting area is Δ E"G"H";(6) Move body again;Supporting area is □ E"F"G"H"

Fig. 9. Leg sequence separated-by-one case fault-tolerant gait.

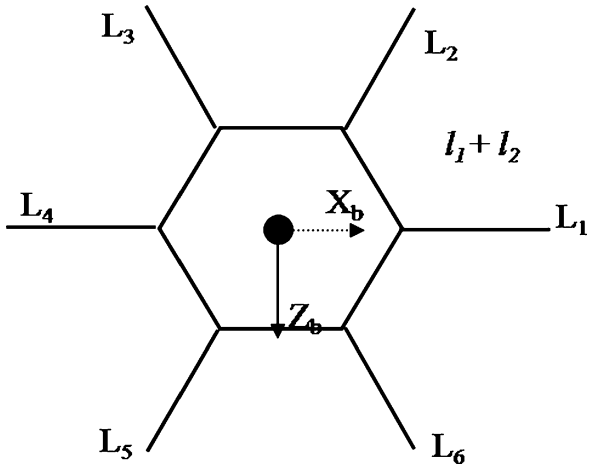

Fig. 10. Body reference frame (top view).

$$\overline{P_4E} = \sqrt{\left((l_1 + l_2) - L\cos\left(\frac{\pi}{3}\right)\right)^2 + \left(L\sin\left(\frac{\pi}{3}\right)\right)^2}, \tag{3}$$

$$\theta_4 = a\tan\left(\frac{L\sin(\frac{\pi}{3})}{(l_1 + l_2) - L\cos(\frac{\pi}{3})}\right), \tag{4}$$

$$\overline{P_5G} = \sqrt{\left(L-(l_1+l_2)\cos\left(\frac{\pi}{3}\right)\right)^2+\left((l_1+l_2)\sin\left(\frac{\pi}{3}\right)-s\right)^2}, \tag{5}$$

$$\theta_5 = \frac{\pi}{6} - a\tan\left(\frac{L-(l_1+l_2)\cos(\frac{\pi}{3})}{(l_1+l_2)\sin\left(\frac{\pi}{3}\right)-s}\right), \tag{6}$$

$$\overline{P_6H} = \sqrt{\left(l_1+l_2-L+R\cos\left(\frac{\pi}{3}\right)\right)^2+\left(R\sin\left(\frac{\pi}{3}\right)-s\right)^2}, \tag{7}$$

$$\theta_6 = \left(\frac{2\pi}{3} - a\tan\left(\frac{R\sin(\frac{\pi}{3})-s}{l_1+l_2-L+R\cos(\frac{\pi}{3})}\right)\right). \tag{8}$$

For the adjacent-legs case, the only difference is for the leg between the two faulty legs, leg 3 for example. The foot tip of leg 3 will move from P_3 to F with the following stride and rotation angle,

$$\overline{P_3F} = \sqrt{\left(l_1 + l_2 - L + R\cos\left(\frac{\pi}{3}\right)\right)^2 + \left(R\sin\left(\frac{\pi}{3}\right)\right)^2}, \tag{9}$$

$$\theta_3 = -\frac{\pi}{3} + a\tan\left(\frac{R\sin(\frac{\pi}{3})}{l_1 + l_2 - L + R\cos(\frac{\pi}{3})}\right). \tag{10}$$

In the above equations, $R\sin(\frac{\pi}{3}) \le L < l_1 + l_2$

D. Loss of more than two legs

If more than two legs are lost, the robot is unable to maintain static stability while walking. Dynamic gaits may still be possible, such as the three-leg dynamics gait of Lee and Hirose.[44] These will not be discussed further here.

5. Terrain Adaptability

The symmetric hexapod robot has different capabilities to deal with rough terrain using different gaits.

5.1. Terrain adaptability with side wave movement

As shown in Fig. 11, a single leg can avoid obstacles or ditches over an area of $[-90°, 90°]$ using a side wave movement. It can overcome an obstacle which is no higher than the length of the calf plus the length of thigh. The width and length of obstacles or ditches are limited to the shaded area in the figure if the body does not move. The lifting leg can overcome wider obstacles and ditches when the robot body is moving.

5.2. Terrain adaptability with kick off movement

Using the kick-off (mammal) gait, the maximum step occurs only when the calf and thigh lie on a straight line (Fig. 12).

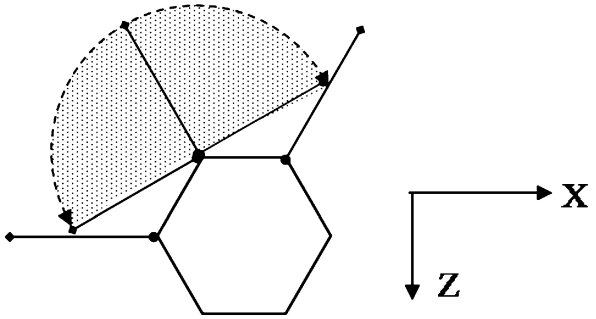

Fig. 11. Terrain adaptability of wave leg.

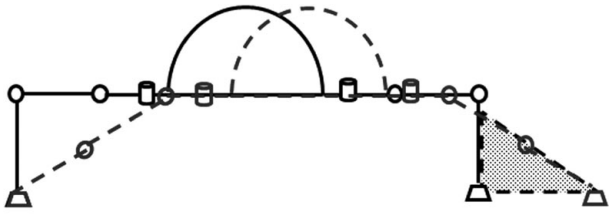

(a)

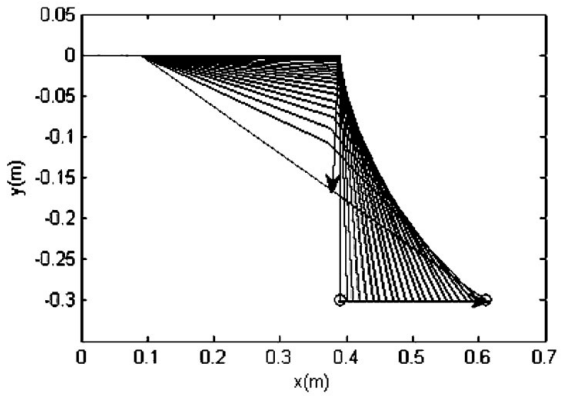

(b)

Fig. 12. Terrain adaptability of kick-off (mammal) leg.

The configuration of obstacles is limited to the shaded area in Fig. 12. Figure 12(b) reveals that, as the stride becomes longer the height under the leg becomes smaller and the obstacle which the mammal leg can overcome becomes lower In summary, the leg walking as in insect wave gait has a greater ability to overcome obstacles or ditches than the mammal/kick-off gait.

5.3. Slope climbing ability

For rigid robots, there are two ways to climb slopes. One ways is keeping the body parallel to ground, the other is keeping the body horizontal, as shown in Fig. 13

For a rigid hexapod robot, gait planning and control are easier using the first method. This is because in the second method the legs will have different trajectories from the flat walking case. However, using the second methods the robot can climb steeper slopes.

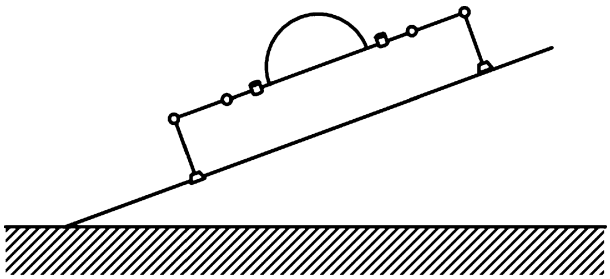

(a) Body parallel to the ground

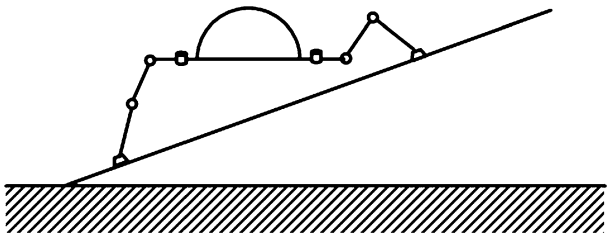

(b) Body horizontal

Fig. 13. Terrain adaptability of kick-off (mammal) leg.

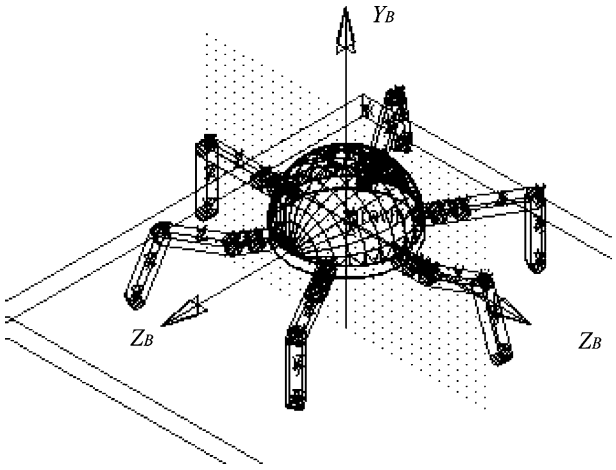

Fig. 14. Body reference frame W_b, 3-open-chains+3-closed-chain.

6. Joined Kinematics and Feet/body Trajectories

6.1. Jointed kinematics

Some studies of the kinematics of multileg robots treat the swing legs and supporting legs separately.[45–52] However, for leg-walking robots, transferring legs' movement depend not only on its three joints but also on the supporting legs. The movements of all legs are related.

Let us assume that the body of the robot is parallel to the ground surface at the initial position. We define three types of system reference frames: the absolute reference frame W_o, body reference frame W_b which is fixed at the mass center of the robot body (Fig. 14), and single leg reference frames W_i (Fig. 15) which are set at the waist joint of the ith leg.

For the body reference frame W_b, initial $X_b(0)$ is parallel to the hip-axis of the leading leg, the origin is at the mass center of the body. For the absolute reference, X_o, Y_o, Z_o are the same as $X_b(0)$, $Y_b(0)$, $Z_b(0)$, the initial direction of the body reference. The origin of absolute reference frame is on the ground, but along the $Y_b(0)$. For the leg reference frame,

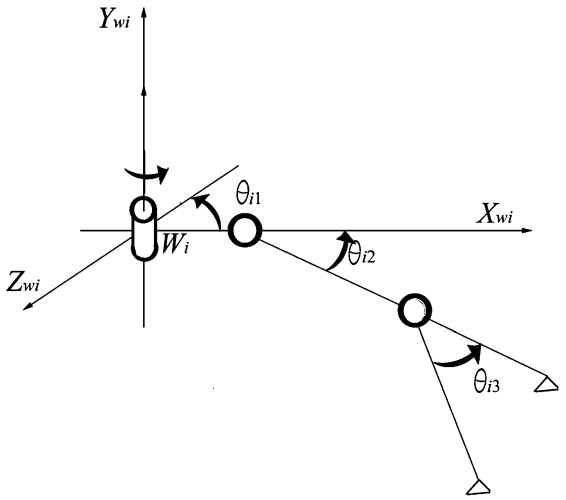

Fig. 15. Leg reference frame W_i.

X_{wi} is along the hip axis; Y_{wi} is along the waist-joint rotate axis, Z_{wi}completes a right-hand frame.

Assume that the body does not rotate during each step. The kinematics of the whole hexagonal hexapod robot is as follows:

$$\begin{cases} r_{fk,o} = \left[J_{b,o}\ {}^{b}_{k}RJ_{Lk,k}\right]\begin{bmatrix}\dot{\theta}_b \\ \dot{\theta}_k\end{bmatrix} = J_{fk,o}\begin{bmatrix}\dot{\theta}_b \\ \dot{\theta}_k\end{bmatrix}, & \text{(11a)} \\ \varpi_{fk,o} = {}^{b}_{k}R\varpi_{fk,k} & \text{(11b)} \end{cases}$$

where k is the number of swing legs; $J_{fk,o}$ denotes the Jacobian matrix of the swing leg in the absolute reference; $\dot{r_{fk,o}}$ is the linear velocity of the swing foot k in the absolute reference frame; $\varpi_{fk,o}$ is the angular velocity of the swing foot k in the absolute reference frame. $\varpi_{fk,o}$ is the angular velocity of the swinging foot k in the leg reference frame W_k (replacing i with k) in Fig. 15; $J_{b,o} = [J_{b1,o}\ \cdots\ J_{bi,o}\ \cdots\ J_{bn,o}\ ]$ is the Jacobian matrix of the body in the absolute reference frame; i is the index specifying the supporting leg; $J_{Lk,k}$ is the Jacobian matrix of the swinging legs in the leg reference frame; ${}^{b}_{i}R$ is the transfer matrix from leg reference to body reference frame, given by

$${}^{b}_{i}R = \begin{bmatrix} \cos(\theta_{oi}) & 0 & \sin(\theta_{oi}) \\ 0 & 1 & 0 \\ -\sin(\theta_{oi}) & 0 & \cos(\theta_{oi}) \end{bmatrix} \quad (12)$$

and $J_{bi,o} = {}^{b}_{i}RJ_{Li,i}$ is the Jacobian matrix of each supporting leg in the global reference frame given by

$$J_{Li,i} = \begin{bmatrix} -(a)s_{i1} & -(b)c_{i1} & l_3c_{i23}c_{i1} \\ 0 & l_2c_{i2} + l_3s_{i23} & l_3s_{i23} \\ -(a)c_{i1} & (b)s_{i1} & -l_3c_{i23}s_{i1} \end{bmatrix} \quad (13)$$

$$a = l_1 + l_2c_{i2} + l_3s_{i23}$$

$$b = l_2s_{i2} - l_3c_{i23}$$

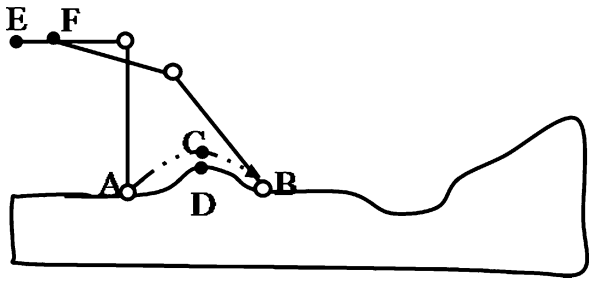

Fig. 16. Trajectory of foot tip.

where'c' denotes 'cosine', 's' denotes 'sine', 'ij' denotes the angle of joint j of leg i; the waist, coxa and knee joint are indexed by 1, 2, 3, respectively with 23 denoting the combination of coax and knee joints; the length of hip, thigh, and calf are denoted by l_1, l_2, l_3, respectively.

6.2. Feet trajectory planning with zero impact walking

When walking on rough terrain and overcoming small obstacles, or changing directions, the trajectories of feet and body of the robot must be planned.

Feet trajectories are designed according to the terrain, shape of obstacles, ditches, holes and stairs, which can be no higher than the calf length.

Connect the initial point A(x_1, y_1, z_1) with end point B(x_3, y_3, z_3) by a straight line. Find the highest point D(x_2, y_2, z_2) above the straight line, and set point C as ($x_2, y_2 + 0.1(y_2 - \min(y_1, y_3)), z_2$) Point C is set higher than point D to avoid collision. A parabolic curve can then be interpolated at A, B, and C as shown in Fig. 16

To avoid impact between feet and the ground, the initial and final velocity and acceleration of the foot-tips as well as the initial and final angular velocities and accelerations of joints are chosen to be zero

The trajectories of the foot-tips, in the absolute reference system are as follows:

$$\begin{cases} dis_{fi,o} = A_{fi}(\phi t - \sin(\phi t)) & \text{(14a)} \\ vel_{fi,o} = A_{fi}(\phi - \phi\cos(\phi t)) & \text{(14b)} \\ acc_{fi,o} = A_{fi}\phi\phi\sin(\phi t)) & \text{(14c)} \end{cases}$$

$$\begin{cases} x_{fi,o} = dis_{fi,o}\cos(\theta_{xz,fi,o}) & \text{(15a)} \\ \dot{x_{fi,o}} = vel_{fi,o}\cos(\theta_{xz,fi,o}) & \text{(15b)} \\ \ddot{x_{fi,o}} = acc_{fi,o}\cos(\theta_{xz,fi,o}) & \text{(15c)} \end{cases}$$

$$\begin{cases} y_{fi,o} = adis^2_{fi,o} + bdis_{fi,o} + c & \text{(16a)} \\ \dot{y_{fi,o}} = (2adis_{fi,o} + b)vel_{fi,o} & \text{(16b)} \\ \ddot{y_{fi,o}} = (2adis_{fi,o} + b)acc_{fi,o} + 2a(vel_{fi,o})^2 & \text{(16c)} \end{cases}$$

$$\begin{cases} z_{fi,o} = dis_{fi,o}\sin(\theta_{xz,fi,o}) & \text{(17a)} \\ \dot{z_{fi,o}} = vel_{fi,o}\sin(\theta_{xz,fi,o}) & \text{(17b)} \\ \ddot{z_{fi,o}} = acc_{fi,o}\sin(\theta_{xz,fi,o}) & \text{(17c)} \end{cases}$$

$$A_{fi} = \frac{L_{sl}}{\sin(\phi\frac{T}{2}) - \phi\frac{T}{2}} \tag{18}$$

$$\phi = 4\frac{\pi}{T}; \tag{19}$$

where: T is the period; ; $L_{sl} = x_3 - x_1$ is the step-length of lifting legs ;$x_{fi,o}$, $y_{fi,o}$ and $z_{fi,o}$ are coordinates of the robot's feet along axes X, Y, and Z in the absolute reference system; a, b, and c are parameters of the parabolic trajectory; $\theta_{xz,fo}$ is the angle between the walking-direction line and axis X on plane $X - Z$.

The equations above represent trajectories in the absolute reference system. If the gravity center of the body keeps the same distance to the ground, the trajectory of foot-tips can be expressed as Eqs. (20)–(24):

$$\begin{cases} dis_{b,o} = A_b(\phi t - \sin(\phi t)) & (20a) \\ vel_{b,o} = A_b(\phi - \phi\cos(\phi t)) & (20b) \\ acc_{b,o} = A_b\phi\phi\sin(\phi t)) & (20c) \end{cases}$$

$$\begin{cases} x_{b,o} = dis_{b,o}\cos(\theta_{xz,b}) & (21a) \\ \dot{x_{b,o}} = vel_{b,o}\cos(\theta_{xz,b}) & (21b) \\ \ddot{x_{b,o}} = acc_{b,o}\cos(\theta_{xz,b}) & (21c) \end{cases}$$

$$\begin{cases} y_{b,o} = 0 & (22a) \\ \dot{y_{b,o}} = 0 & (22b) \\ \ddot{y_{b,o}} = 0 & (22c) \end{cases}$$

$$\begin{cases} z_{b,o} = -dis_{b,o}\sin(\theta_{xz,b}) & (23a) \\ \dot{z_{b,o}} = -vel_{b,o}\sin(\theta_{xz,b}) & (23b) \\ \ddot{z_{b,o}} = -acc_{b,o}\sin(\theta_{xz,b}) & (23c) \end{cases}$$

$$A_b = \frac{L\_step}{\sin(\phi\frac{T}{2}) - \phi\frac{T}{2}}, \tag{24}$$

where, L_step is the stride of the body in half T; x_b, y_b and z_b are the coordinates of the position of robot's body along axes X, Y, and Z in the absolute reference system; $\theta_{xz,b}$ is the angle between body trajectory and the X-axis. If the trajectory of the body is a straight line, both $\dot{\theta_{xz,b}}$ and $\frac{d(\cos(\theta_{xz,b})\dot{\theta_{xz,b}}}{dt}$ will be zero. Other parameters are same as in Eqs. (14)–(17).

6.3. Stride selection

The problem of stride optimization did not receive great attention in literature. Some researchers tried to implement the robot gait with the maximum stride achievable by the leg.[3,6] However, using the maximum stride is unnecessary and inefficient in some situations according to the analysis we report in the following.

Figure 17 depicts the rotation angle of knee and coax joints as a function of stride while the leg protrudes as in mammal gait. The maximum stride for a mammal protruding leg of NOROS is about 22 cm, as stated in Table II The angular

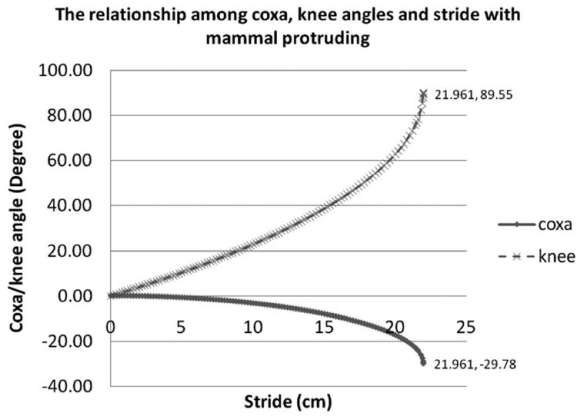

(a)

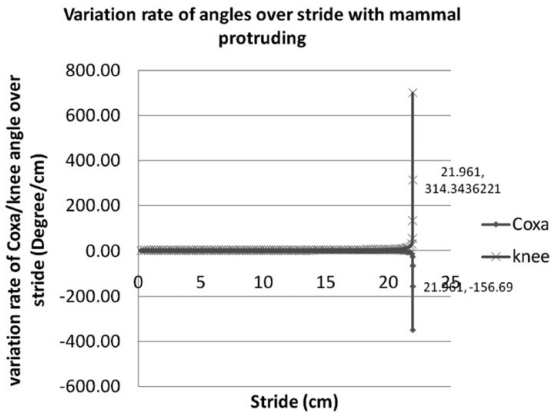

(b)

Fig. 17. Stride of mammal gait protruding.

variation rates of coxa and knee over stride increase suddenly after the stride reaches around 21.9 cm, passing from less than $10^\circ/cm$ to more than $200^\circ/cm$, as shown in Fig. 17(b). Empirically, 20 cm can be a good solution for the mammal protruding stride. At 20 cm the angular variation rates of coxa and knee are only -2.88°/cm and 6.78°/cm respectively, much less than -14.5°/cm and 30°/cm at 21.9 cm. During mammal retracting the changing rate of coxa increases with the stride while the one of knee decreases. Nevertheless, both changing rates are small even the retracting stride reaches high values as 28 cm (Fig. 18). Therefore, it is useful to optimize the stride selection in the mammal gait when legs are protruding but not while retracting.

According to Table II in Section 3, in the insect wave gait of NOROS, the stride can reach 14.57 cm without losing static stability. In such gait, the of the coax joint changes less than 1° and the knee joint angle changes a little from 0° to 6.8° (Fig. 19). Consequently, it is unnecessary to optimize the stride selection for insect walking under static stability. For the mammal gait, to produce the same stride, the waist joint angle is 0°, the coax joint angle changes from 0° to 7.5°, the knee joint angle approaches 37°. To retract the same stride, the waist joint angle is 0°, the coxa joint angle changes from 0° to 7°, the knee joint angle approaches about 28°. For same stride, the angular velocities of the mammal gait are much higher than in the insect wave gait.

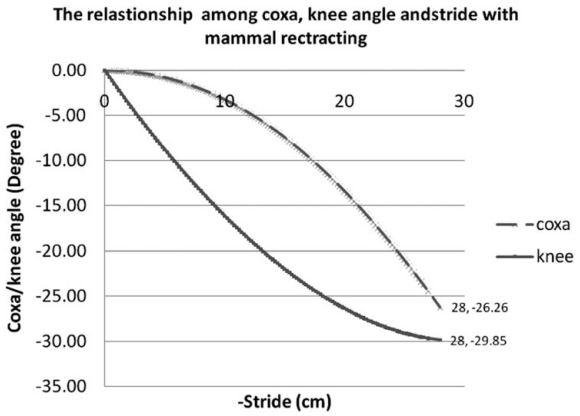

(a)

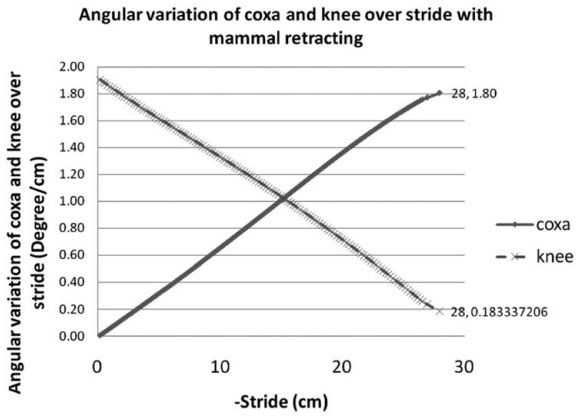

(b)

Fig. 18. Strider of mammal gait retracting.

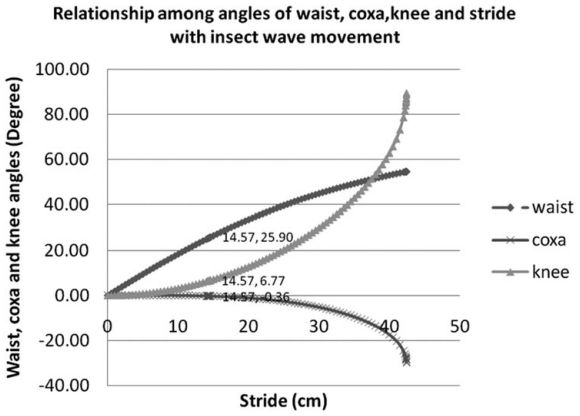

Fig. 19. Relationship among joint-angles and stride of insect gait.

Table III. Parameters of Prototype.

	Each leg			
	Hip	Thigh	Calf	Body
Mass (kg)	0.11	0.25	0.09	0.30
Length (cm)	$l_1 = 3$	$l_2 = 7$	$l_3 = 13$	R = 13.7

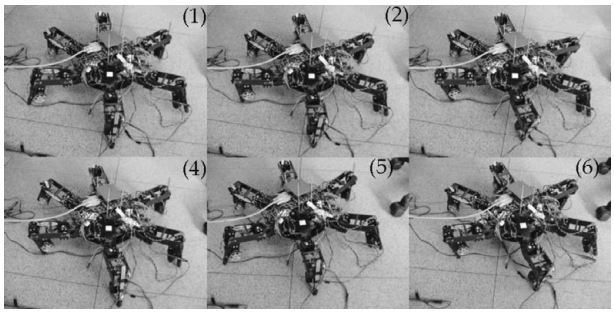

Fig. 20. 3+3 mix-gait.

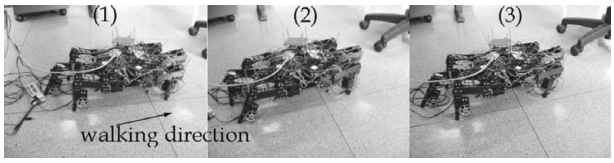

Fig. 21. 3+3 mammal-gait.

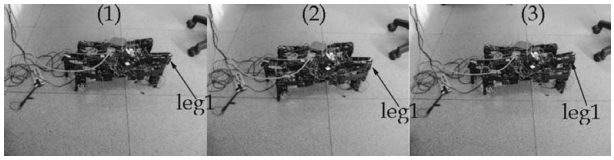

Fig. 22. 3+3 insect-gait.

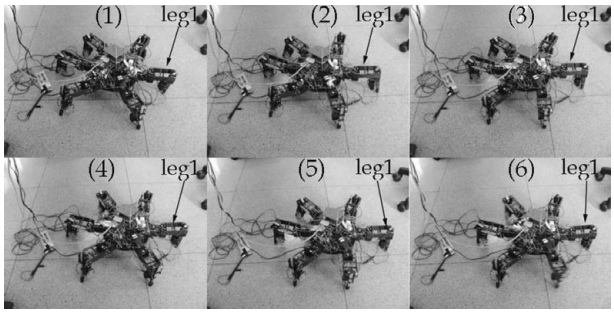

Fig. 23. 4+2 gait.

7. Experiments

Experimental studies were performed for most of the aforementioned gaits using the old prototype from Ladyfly since the prototype of new design is under construction. The current prototype is about one-third-scale of our previous design and its calf is not as long as the thigh. The physical parameters for this prototype are as given in Table III. Note that the thigh of this prototype is relatively shorter than our design, whereas its calf is relatively longer.

Each leg has three revolute joints actuated by position controlled servo-motors. An onboard micro-controller (MINI-ABB+SSC32 with Basic Atom PRO) was installed. Both wired and wireless communications are available. Wi-Fi 802.11b is used for wireless communication.

The normal 3+3 and 4+2 gaits were successfully tested (Fig. 20–23).

During the experiments, we found that the mixed gait was the most stable, followed by the mammal gait and then insect gait is the least stable. For the maximum possible stride, the longest was from the mammal gait, then the mixed gait and lastly the insect gait. The longest stride for the insect gait is nearly half that of the mammal gait, as suggested in Table II.

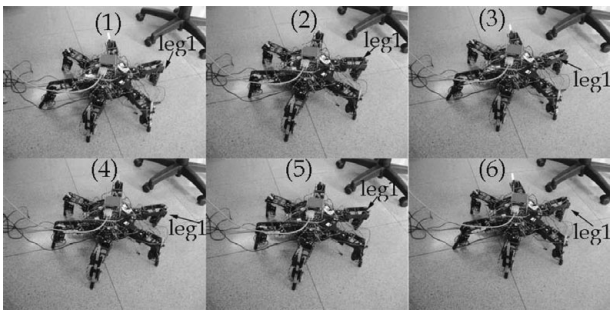

Fig. 24. Turn left with 20° by mix-gait.

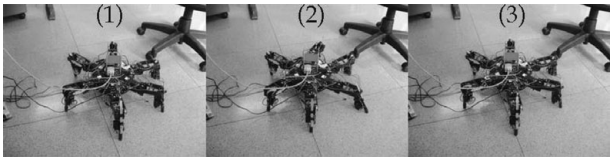

Fig. 25. Turn left 120° by mix-gait.

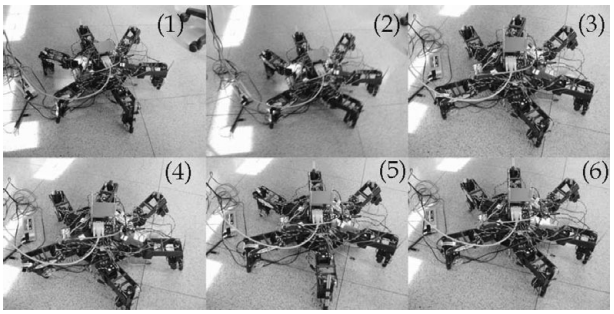

Fig. 26. The 5-leg-gait while leg 1 broken.

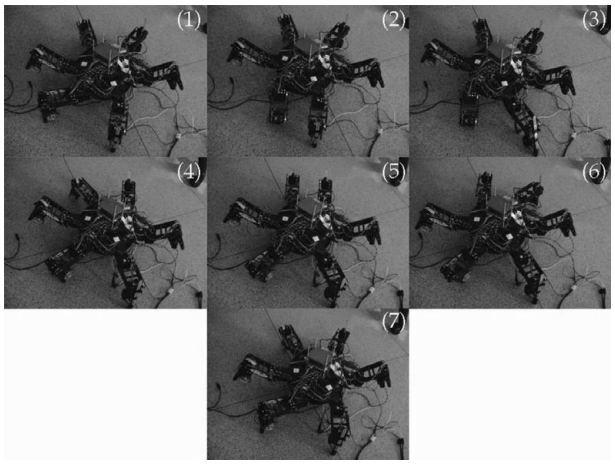

Fig. 27. The 4-leg-gait while two opposite legs (1 and 4) broken.

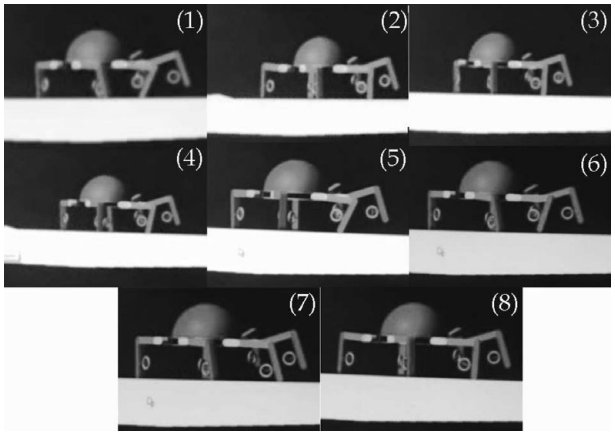

Fig. 28. Fault-tolerant gait of two adjacent legs losing.

For the current prototype, the maximum possible stride of the insect gait is less than 3 cm, while for the mammal gait, it can reach 7 cm.

The turning experiments were also conducted for each gait. Small angle $(-30^\circ, 30^\circ)$ turning could be achieved easily by adjusting the crab angle for all mammal and mixed gaits. Figure 24 displays a left turn of 20° using the mixed gait. Special angle $(n \cdot 60^\circ, n = 1, 2...5)$ turning by mixed gait was achieved by changing the leading leg (leg 2, leg 3 . . . leg 6). Figure 25 informs the turning by 120° using the mixed gait. Other angles' turnings were reached by changing the leading leg together with appropriate adjustment of the crab angle. For example, to make a 100° turn, use leg 3 as the leading leg with crab angle $+20^\circ$.

For the current prototype, it is difficult to turn through the insect gait. During our experiments, turning by the insect gait always made the prototype fallen down, unless a very small stride was used, could turning be achieved. The mixed gait is the most stable in tripod gaits because of the large supporting areas. The 4+2 mixed gait is even more stable. However, the continuous mixed tripod gait is more efficient than 4+2 mixed gait as their duty factors are 0.5 and 0.75 respectively.

Fault-tolerant gaits were tested successfully with loss of one leg lost (Fig. 26) and loss of two legs (Fig. 27–29).

For the case of loss of two legs, seven steps were needed for one walking period (Fig. 27): transferring right rear leg, transferring right front leg, then moving body the first time, transferring left rear leg, transferring left front leg, finally moving body the second time.

For the cases of loss of two adjacent legs and two legs that are separated by one, simulation in ADAMS controlled through MATLAB were performed with our new design because servo-motors installed on the current prototype were not powerful enough to realize those gaits. For all simulations, the parameters of digital model are from Table I in Section 2.

The experiments for overcoming obstacles were also successful, as demonstrated by overcoming a 3 cm plate and 8 cm book as shown in Fig. 30. The prototype could overcome the same height as the length of the calf.

Conclusion

In this paper, the locomotion of symmetric hexapods has been studied in detail and tested mostly on a NOROS prototype We have presented a comprehensive study of hexagonal hexapod gaits including normal and fault-tolerant ones. Gaits of rectangular and hexagonal six-legged robots have been compared from several aspects: stability, fault tolerance, terrain adaptability, and walking ability. To facilitate simulations and experiments we have provided

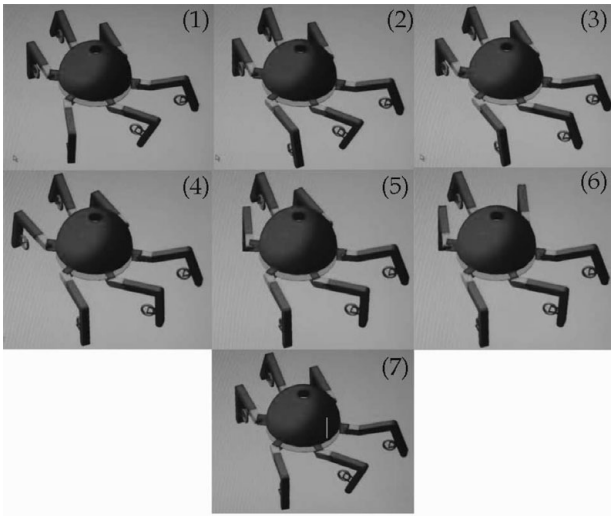

Fig. 29. Fault-tolerant gait of two meta-legs losing.

Fig. 30. Prototype overtaking a book with 3+3 mix-gait.

integrated kinematics of swinging and supporting legs for continuous gaits.

Hexagonal hexapod robots have been shown to be more flexible than rectangular ones. Moreover, hexagonal hexapods have many feasible gaits. In addition to the well-known insect gait and mammal gait, a new mixed gait for hexagonal six-legged robots has been proposed in the paper which entails some features of both insect and mammal gaits. Except classified by legs movement as mentioned above, hexapod robots gaits are categorized according to the number of supporting legs during walking, as $3+3$ tripod, $4+2$ fault-tolerant quadruped, and $5+1$ one by one gaits. On account to the introduction of mixed gait, each numbered gait has one more form. Among three tripod gait forms, the most stable is the mixed one. The mammal gait can reach the longest stride; whereas the continuous insect gait has the shortest maximum stride and poorest stability. However, the side-wave gait can overtake higher obstacles than the mammal kick-off movement. Finally, we have discovered that walking with the longest stride is not optimal, especially for the mammal kick-off gait.

Thanks to their six legs, hexapod robots have redundancy and fault tolerance. Gaits where one leg is lost or two opposite legs are lost have been discussed in recent times. In this paper we have tackled also the cases in which two adjacent legs or two separated by a normal leg are damaged. Algorithms for realizing these two fault-tolerant gaits have been detailed and validated with simulations.

From experiments we have found that, for the quadruped fault-tolerant gaits under consideration, it will be more stable if the length of hip plus thigh is larger than radius of the body.

The results presented in this paper contribute to intelligent locomotion for symmetric six-legged robots. Possible applications include using multilegged robots over off-road terrain, such as for planetary exploration. Our results on for fault-tolerant gaits could multilegged robots to use some of legs as arms to perform useful operations. Future works should be focused on the study of energy cost of different gaits, dynamic gaits, intelligent walking, and operations on lunar surface.

Acknowledgments

Thanks to the China NSFC (Grant no. 50720135503), H-Tech Research and Development Program of China (863 Program: Grant no. 2006AA04Z207), and the S&T cooperation program (2006–2009) of the Governments of China and Italy for financial support to researchers exchange. Thanks for the support to the Laboratory of Robotics ARIAL of Politecnico di Milano for the realization of NOROS prototype and the development of tests, with the support of all the team. Great gratitude to Prof. Chen I-Ming of Nanyang Technological University and Dr. Jon Selig of London South Bank University for their kind suggestions on the final organization of this paper and English improvement. We also thank Prof. J.Jim Zhu from Ohio University and Dr. Daniele Perissin from Politecnico di Milano for helping improving English in revision.

References

1. A. Rovetta and E. C. Paul, "New Robot Concept for Mars Soil Exploration: Mechanics and Functionality," *ASTRA 2004, Eighth ESA Workshop on Advanced Space Technologies for Robotics and Automatian,* Nordwijk, The Netherlands (Nov. 2–4 , 2004) pp. 1–8.
2. A. Preumont, P. Alexadre and D. Ghuys, "Gait Analysis and Implementation of a Six Leg Walking Machine," *91ICAR, Fifth International Conference on Advanced Robotics 'Robots in Unstructured Environments*,' Pisa, Italy, Vol. 2 (Jun. 19–22, 1991) pp. 941–945.
3. J.-M. Yang and J.-H. Kim, "A Strategy of Optimal Fault Tolerant Gait for the Hexapod Robot in Crab Walking," *IEEE International Conference on Robotics and Automation,* Leuven, Belgium, Vol. 2 (May 16–20, 1998) pp. 1695–1700.
4. J.-M. Yang and J.-H. Kim, "Fault Tolerant Locomotion of the Hexapod Robot," *IEEE Transactions on System, Man and Cybernetics*, Vol. 28(1) (Feb. 1998) pp. 109–116.
5. J.-M. Yang, "Fault-Tolerant Gait Generation for Locked Joint Failures," *IEEE International Conference on Systems, Man and Cybernetics,* Washington D.C., USA, Vol. 3 (Oct. 5–8, 2003) pp. 2237–2242.
6. J.-M. Yang and J.-H. Kim, "Optimal Fault Tolerant Gait Sequence of the Hexapod Robot with Overlapping Reachable Areas and Crab Walking," *IEEE Transactions on System, Man and Cybernetics, Part A,* Vol. 29(2) (Mar. 1999) pp. 224–235.
7. J.-M. Yang and J.-H. Kim, "A Fault Tolerant Gait for a Hexapod Robot over Uneven Terrain," *IEEE Transactions on Systems, Man, and Cybernetics—part b: Cybernetics*, Vol. 30 (1) (Feb. 2000) pp. 172–180.
8. N. Koyachi, T. Arai, H. Adachi, K. Asami and Y. Itoh, "Hexapod with Integrated Limb Mechanism of Leg and Arm," *IEEE International Conference on Robotics and Automation,* Nagova, Japan, Vol. 2 (May 21–27, 1995) pp. 1952–1957.
9. Y. Takahashi, T. Arai, Y. Mae, K. Inoue and N. Koyachi, "Development of Multi-Limb Robot with Omnidirectional

Manipulability and Mobility," *Proceedings of the 2000 IEEE-RSJ International Conference on intelligent Robots and Systems*, Takamatsu, Japan, Vol. 3 (31 Oct.–5 Nov., 2000) pp. 2012–2017.
10. J. Bares and M. Hebert, T. Kanade, E. Krotkov, T. Mitchell, R. Simmons and W. Whittaker, "Ambler—An Autonomous Rover for Planetary Exploration," *IEEE Computer* (1989) pp. 18–26.
11. M. Kaneko, M. Abe and K. Tanie, "A hexapod walking machine with decoupled freedoms," *IEEE J. Robot. Autom.* **RA-1**(4), 183–190 (Dec. 1985).
12. W.-J Lee and D. E. Orin, "Omni-directional supervisory control of a multi-legged vehicle using periodic gait," *IEEE J.* Robot. Autom. **4**(6), 635–642 (Dec. 1988).
13. E. Krotkov and J. Bares *et al.*,"Ambler: A Six-Legged Planetary Rover," *Fifth international conference on advanced robotics-91 ICAR,* Pisa, Italy (1991) pp. 717–722.
14. D. Wettergreen, H. Thomas and C. Thorpe, "Planning Strategies for the Ambler Walking Robot," *IEEE International Conference on Systems Engineering*, Pittsburgh, PA, USA (Aug. 9–11, 1990) pp. 198–203.
15. S. Hirose, K. Homma, S. Matsuzawa and S. Hayakawa, "Parallel Link Walking Vehicle and Its Basic Experiments (in Japanese)," *Sixth Symposium on Intelligent Mobile Robots*, (1992) pp. 7–8.
16. Y. Ota, Y. Inagaki, K. Yoneda and S. Hiros, "Research on a Six-Legged Walking Robot with Parallel Mechanism," *Proceedings of the 1998 IEE WRSJ Intl. Conference on Intelligent Robots and Systems*, Victoria, BC, Canada (Oct. 1998) pp. 241–248.
17. H. B. Gurocak and J. Peabody, "Design of a robot that walks in any direction," *J. Robot. Syst.* **15**(2), 75–83 (1998).
18. B.-H. Lee and I.-K. Lee, "The Implementation of the Gaits and Body Structure for Hexapod Robot," *ISIE 2001. IEEE International Symposium on Industrial Electronics,* Pusan, South Korea, Vol. 3 (Jun. 12–16, 2001) pp. 1959–1964.
19. U. Saranli, M. Buehler and D. E. Koditschek, "RHex: A simple and highly mobile hexapod robot," *Int. J. Robot. Res.* **20**(7), 616–631 (Jul. 2001).
20. T. T. Lee, C. M. Liao and T. K. Chen, "On the stability properties of hexapod tripod gait," *IEEE J. Robot. Autom.* **4**(4),427–434 (Aug. 1988).
21. S. M. Song and B. S. Choi, "The optimally stable ranges of 2n-legged wave gaits," *IEEE Trans. Syst. Man Cybern.—part b: Cybern.* **20**(4), 888–902 (Jul.–Aug. 1990).
22. X.-J.Wang, "A Study of Locomotion and Force Planning for Multilegged Walking Robots," *Ph.D. Thesis (in Chinese),* (Wuhan, P.R. China: Huazhong University of Science & Technology, Oct. 2005) pp. 95–100.
23. J. Su, "The Research of the Gait Planning and Control of the Multilegged Walking Robot," *Master Thesis (in Chinese)* (Wuhan, P.R.China: Huazhong University of Science & Technology, Apr. 2004).
24. Q.-J. Huang and K. Nonami, "Humanitarian mine detecting six-legged walking robot and hybrid neuro walking control with position/force control," *Mechatronics* **13**, 773–790 (2003).
25. E. I. Kugushev and V. S. Jaroshevskij, "Problem of Selecting a Gait for an Integrated Locomotion Robot," *Process Fourth International conference. Artificial Intelligence,* Tbilisi, Georgian SSR, USSR (Sep. 1975) pp. 789–793.
26. R. B. McGhee and G. I. Iswandhi, "Adaptive locomotion of a multilegged robot over rough terrain," *IEEE Trans. Syst. Man Cybern.* **SMC-9**(4), 176–182 (Apr. 1979).
27. J. M. Porta and E. Celaya, "Reactive free gait generation to follow arbitrary trajectories with a hexapod robot," *Robot. Auton. Syst.* **47,** 187–201 (2004).
28. M. S. Erden and K. Leblebicioğu, "Free gait generation with reinforcement learning for a six-legged robot," *Robot. Auton. Syst.* **56**, 199–212 (2008).
29. K. Kamikawa, T. Arai, K. Inoue and Y. Mae, "Omni-Directional Gait of Multi-Legged Rescue Robot," *Proceedings of the 2004 IEEE International Conference on Robotics and Automation*, New Orleans, LA - 4111 (2004) pp. 2171–2176.
30. K. Yoneda and K. Suzuki, "Gait and foot trajectory planning for versatile motions of a six-legged robot,"*J. Robot. Syst.* **14**(2), 121–133 (1997).
31. S. K.-K. Chu and G. K.-H. Pang, "Comparison between different model of hexapod robot in fault-tolerant gait,"*IEEE Trans. Syst. Man. Cybern. Part A* **32**(6), 752–756 (Nov. 2002).
32. P. Gonzalez de Santos, J. A. Cobano, E. Garcia, J. Estremera and M. A. Armada, "A six-legged robot-based system for humanitarian demining missions," *Mechatronics* **17**, 417–430 (2007).
33. P. Gonzalez de Santos, E. Garcia and J. Estremera, "Improving walking-robot performances by optimizing leg distribution," *Auton. Robots* **23**(4), 247–258 (2007).
34. A. Rovetta and X. Ding, "Next Steps for Robotic Landers Rovers and Outposts," *ILEWG 2006*, Beijing, China (Jul. 2006) pp. 23–27.
35. A. Rovetta, "New Progress on the Novel Robotics Systems for Moon Exploration," *Ilewg 2007*, Sorrento, Italy (24–26 Oct. 2006).
36. Z.-Y.Wang, X.-L. Ding and A. Rovetta, "Structure Design and Locomotion Analysis of a Novel Robot for Lunar Exploration," *Twelfth IFToMM World Congress*, Besançon, France (Jun. 2007) pp. 18–21.
37. A. Rovetta and E. C. Paul, "Design Methodologies for a Colony of Autonomous Space Robot Explorers," *Intelligence for Space Robotics*(A. Howard and E. d. Tunstel, eds.), (TSI Press Series, 2006) pp. 93–112.
38. J. J. Chen, A. M. Peattie, K. Autumn and R. J. Full, "Differential leg function in a sprawled-posture quadrupedal trotter," *J. Exp. Biol.* **209**, 249–259 (2006).
39. S. Hirose and F. Martins, "Generalized standard leg trajectory for quadruped waking vehiche," *Trans. Soc. Instrum. Control Eng.* **25**(4),455–46 (1989).
40. K. Tsujita, K. Tsuchiya and A. Onat, "Adaptive gait pattern control of a quadruped locomotion robot," *2001 IEEE/RSJ International Conference on Intelligent Robots and Systems*, Hawaii, USA, Vol. 4 (29 Oct.–3 Nov. 2001) pp. 2318–2325.
41. X.-D. Chen, Y. Su and W.-C. Jian, "Motion Planning and Control of Multilegged Walking Robots," *Huazhong University of Science and Technology Press (in Chinese)*, Wuhan, China (Jun. 2006).
42. J. Estremera and P. Gonzalez de Santos, "Free gaits for quadruped robots over irregular terrain," *Int J Robot. Res.* **21**(2), 115–130 (Feb. 2002).
43. J. Estremera and P. Gonzalez de Santos, "Generating continuous free crab gaits for quadruped robots on irregular terrain," *IEEE Trans. Robot.* **21**(6), 1067–1076 (Dec. 2005).
44. Y.-J. Lee and S. Hirose, "Three-Legged Walking for Fault Tolerant Locomotion of a Quadruped Robot with Demining Mission," *2000 IEEE/RSJ International Conference on Intelligent Robots and Systems(IROS 2000)*, Takamatsu, Japan, Vol. 2 (31 Oct.–5 Nov. 2000) pp. 973–978.
45. C. A. Berardi-Gonziilez and H. Martinez-Alfaro, "Kinematic Simulator for an Insect-Like Robot," *IEEE International Conference on Systems, Man and Cybernetics*, Washington DC, USA, Vol. 2 (2003) pp. 1846–1851.
46. W.-J. Lee and D. E. Orin, "The kinematics of motion planning for multilegged vehicles over uneven terrain Lee," *Robot. Autom. (see also IEEE Trans. Robot. Autom.)* **4**(2), 204–212 (1988).
47. J. P. Barreto, A. Trigo, P. Menezes, J. Dias and A. T. De Almeida , "FED-the Free Body Diagram Method. Kinematic and Dynamic Modeling of a Six Leg Robot, "*Advanced Motion Control (AMC'98)*, Coimbra, Portugal (29 Jun.–1 Jul. 1998) pp. 423–428.
48. A. Shkolnik and R. Tedrake, "Inverse Kinematics for a Point-Foot Quadruped Robot with Dynamic Redundancy

Resolution," *2007 IEEE International Conference on Robotics and Automation,* Roma, Italy (10–14 Apr. 2007) pp. 4331–4336.
49. W.-J. Chen, S. H. Yao and K. H. Low, "Modular Formulation for Dynamics of Multi-Legged Robots," *Eighth International Conference on Advanced Robotics (ICAR'97)*, Monterey, CA, USA (7–9 Jul. 1997) pp. 279–284.
50. M. S. Erden and K. Leblebicioğu, "Torque Distribution in a Six-Legged Robot," *IEEE Trans. Robot.* **23**(1), 179–186 (2007).
51. D. W. Marhefka and D. E. Orin, "Quadratic Optimization of Force Distribution in Walking Machines," *Proceedings of the 1998 IEEE International Conference on Robotics & Automation*, Leuven, Belgium (May 1998) pp. 477–483.
52. M. F. Silva, J. A. Tenreiro Machado and A. M. Lopes, "Performance Analysis of Multi-Legged Systems," *International Conference on Robotics 8 Automation*, Washington, DC (May 2002) pp. 2234–2239.